# Joint Optimization Algorithm for Network Reconfiguration and Reactive Power Control of Wind Farm in Distribution System

JINGJING ZHAO, XIN LI,JIPING LU,CONGLI ZHANG
State Key Laboratory of Power Transmission Equipment & System Security and New Technology
Chongqing University
400030 Chongqing
CHINA
jingjingzhao@cqu.edu.cn

*Abstract:* -In recent years, the number of small size wind farms used as DG sources located within the distribution system are rapidly increasing. Wind farm made up with doubly fed induction generators (DFIG) is proposed in this paper as the continuous reactive power source to support system voltage control due to the reactive power control capability of DFIG. In the distribution system, considering network reconfiguration and wind farm reactive power control are both used to improve power profile and they have an inherent coupling relationship, in this paper, a joint optimization algorithm of combining reactive power control of wind farm and network reconfiguration is proposed. In the proposed joint optimization algorithm, an improved hybrid particle swarm optimization with wavelet mutation algorithm (HPSOWM) is developed for voltage profile improvement which utilized reactive power output of wind farm as the control variable. In each particle updating instance at each iteration of reactive power output optimization algorithm, a binary particle swarm optimization algorithm (BPSO) is utilized to find the optimal network structure. Finally, 16-node feeder is used as a test case to evaluate the algorithm. The experimental result demonstrates the correctness of the algorithm.

*Key-Words:* - wind farm, DFIG wind turbine, reactive power control, network reconfiguration, particle swarm optimization

## 1 Introduction

Currently, there is an increasing concern over the environmental impact and sustainability of traditional fossil-fueled power plants. Because wind energy is one of the most important and promising renewable energy resources in the world, leading to a growing penetration of the wind energy in electrical system[1-4]. As a consequence, the number of small size wind farms used as DG sources located within the distribution system is rapidly increasing in recent years. Installing wind farm in the distribution system can defer the investments for the distribution system expansion, but at the same time, the power quality of the distribution network has to be ensured. Hence, wind farms are more and more required to take part in the control of electric variables and in particular in reactive power control [5, 11].

The variable-speed wind turbine equipped with doubly fed induction generators (DFIG) is the most employed generator for the recently built wind farm. The DFIG is able to obtain the maximum active power from wind speed and the generated reactive power can be controlled in an independent way[6-8]. Utilizing DFIG reactive power control capability, wind farm made up with DFIG can be used as the continuous reactive power source to support system voltage control with fewer costs on the reactive power compensation device.

Regarding DFIG, great variety of control strategies can be used in the operation of DFIG and has been described in several works [9]–[12]. In these works, strategies to control active and reactive power wind farm outputs also were proposed. Ref. [9] propose a detailed mathematical model of the DFIG and two alternative simulation models for the analysis of both the active and reactive power performances associated with a wind farm constituted exclusively by DFIG. Ref. [10] proposes an optimized dispatch control strategy for active and reactive powers delivered by a doubly fed induction generator in a wind park. Ref. [11] presents a control strategy developed for the reactive power regulation of wind farms made up with DFIG, in order to contribute to the voltage regulation of the electrical grid to which farms are connected. Ref. [12] describes the relation between active and reactive power in order to keep each DFIG operating inside the maximum stator and rotor currents and the steady state stability limit. Ref. [13] describes an operational optimization strategy to be adopted at the wind farm control level that enables defining the commitment of wind turbines and their active and reactive power outputs. Network reconfiguration is one of the most significant control schemes in the distribution system, which alter the topological structure of distribution feeders by changing open/closed status of sectionalizing and tie switches to reduce the system real power losses and to improve voltage profiles. Network reconfiguration achieves this goal by optimizing active power flow in the system while wind farm reactive power control achieves this goal by reducing reactive power flow in the system. It is clear that there is an inherent coupling relationship between network reconfiguration and wind farm reactive power control. They will strengthen each other in the combination of these two means for better optimization results in distribution systems. Therefore, there is a need to find the optimal wind farm reactive power output and the optimal network structure.

In this paper, Wind farm made up with DFIG is proposed as the continuous reactive power source to support system voltage control due to the reactive power control capability of DFIG. A joint optimization algorithm of combining wind farm reactive power output and network reconfiguration to minimize the real power loss of the system and the deviation of the bus voltage is proposed. To achieve high performance and high efficiency of the proposed algorithm, an improved hybrid particle swarm optimization with wavelet mutation algorithm (HPSOWM) is utilized to find the optimal reactive power output of wind farm, and a binary particle swarm optimization algorithm (BPSO) is developed to find the optimal network structure for each particle updating instance at each iteration of wind farm reactive power output optimization algorithm.

To concentrate on developing an efficient joint optimization algorithm to find the optimal wind farm reactive power output and network configuration given measured load levels, we assume that telemetered system demand and configuration data are available as part of a distribution automation system and that wind farm reactive power output and reconfiguration switches can be remotely controlled [14].

## 2 System model and control

### 2.1 DFIG wind turbine model

Fig.1 shows the model of DFIG consisting of a pitch controlled wind turbine and an induction generator[15]. The stator of the DFIG is directly connected to the grid, while the rotor is connected to a converter consisting of two back-to-back PWM inverters, which allows direct control of the rotor currents. Direct control of the rotor currents allows for variable speed operation and reactive power control thus DFIG can operate at a higher efficiency over a wide range of wind speeds and help provide voltage support for the grid. These characteristics make the DFIG ideal for use as a wind generator.

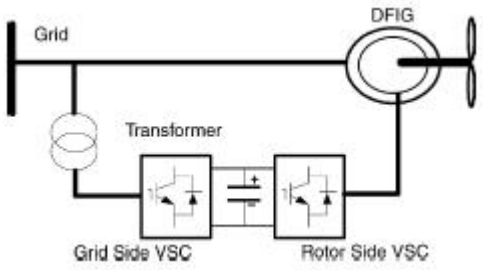


Fig.1 DFIG wind turbine

Generally, the reference value of the active power that a DFIG should generate is established through optimum generation curves, which provide the active power as a function of the generator rotational speed. Such curves are derived as a result of through analysis of the wind turbine aerodynamics, and define the maximum mechanical power the DFIG can extract from the wind at any angular speed [9, 13].

Fig.2 shows a typical power curve for a 660kW DFIG wind turbine [15]. When the active power generated by the DFIG is fixed following a specific optimum generation curve, the reactive power generated or absorbed by a DFIG should take into account the capability limits of the DFIG.

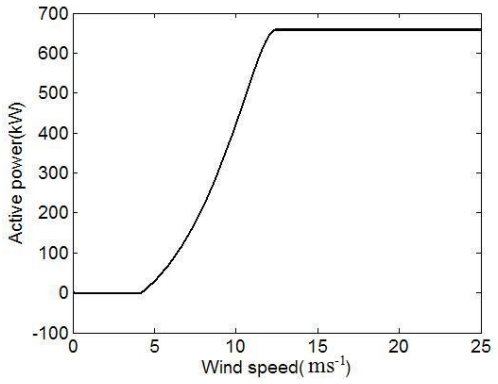


Fig.2 Power curve of a 660kW DFIG wind turbine

## 2.2 DFIG capability limits curve

Fig. 3 shows the single-phase equivalent circuit of the DFIG. Where $U_S$ is the stator voltage, UR the rotor voltage, $I_S$ the stator current, $I_R$ the rotor current, $R_S$ the stator resistance, $R_R$ the rotor resistance, $X_S$ the stator reactance, $X_R$ the rotor reactance, $X_M$ the mutual reactance, and s is the slip.

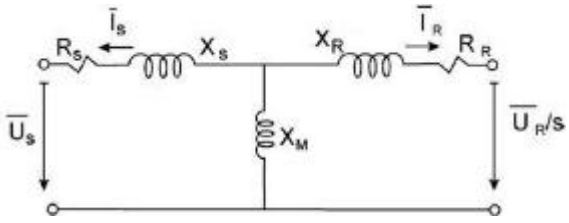


Fig.3. DFIG equivalent circuit

In Ref. [12], power capability limits of DFIG have been studied. The stator active and reactive power is expressed as a function of stator current and rotor current:

$$P_S^2 + Q_S^2 = (3U_S I_S)^2 \quad (1)$$

$$P_S^2 + (Q_S + 3\frac{U_S^2}{X_S})^2 = (3\frac{X_M}{X_S}U_S I_R)^2 \quad (2)$$

In the PQ plane, equation (1) represents a circumference centered at the origin with radius equal to the stator rated apparent power. Equation (2) represents a circumference centered at $[-3U_S^2/X_S, 0]$ and radius equal to $3U_S I_R X_M/X_S$. Therefore, given a maximum permissible value for stator current IS and rotor current IR allowed by DFIG, once the active power to be generated is fixed following a specific optimum generation curve, the limit for reactive power dependent of the stator voltage and the active power is generated.

Fig.4 shows the composed curve for the DFIG total capability limits. Additionally, the steady state stability limit of the DFIG is taken into account, which represented as vertical line at the $[-3U_S^2/X_S, 0]$ coordinate in Fig.4. Rotor reactive power is not taken into account because it cannot flow through the power converter cascade.

## 2.3. Wind farm model

In this paper, a wind farm model is developed with n DFIG wind turbines connected in parallel. The wind speed at each wind turbine is considered to be the same and therefore they generate the same output power. As a result, the total active and

reactive power output of the wind farm equal to the sum of the active and reactive power generated by each of the DFIG wind turbine in the wind farm:

$$P_{WF} = \sum_{i=1}^{n} P_{gi} \quad (3)$$

$$Q_{WF} = \sum_{i=1}^{n} Q_{gi} \quad (4)$$

where PWF represents the active power output of the wind farm, QWF represents the reactive power output of the wind farm, $P_{gi}$ represents the generated active power of each *i* DFIG and $Q_{gi}$ represents the generated or absorbed reactive power of each *i* DFIG.

### 2.4 Load flow including wind farm

In this paper, node integrating DFIG based wind farm is treated as PQ nodes in a load flow analysis. In situations where the wind speed at wind farm is specified and the loads at buses are known, the real power output of DFIG can be calculated by means of the power curve. Knowing the active of the each DFIG, the active power of the wind farm is gained. The reactive power of the wind farm is obtained from the optimization algorithm proposed in this paper. Then a backward-forward load flow algorithm is utilized to determine the real and reactive current injection at all the buses. Using these currents and a backward-forward sweep scheme the branch currents are found and voltages at all the buses are updated for this iteration.

## 3. Problem formulation

In this section, wind farm reactive power control and network reconfiguration joint optimization has been modeled as a multi objective, non differentiable optimization problem. In the proposed joint optimization algorithm, the objective function consists of two terms: 1) the real power loss of the system, 2) the deviation of the bus voltage.

$$\min f_1(\overline{X}) = \lambda_1 \sum_{i=1}^{Nl} R_i \frac{P_i^2 + Q_i^2}{|V_i|^2} + \lambda_2 \max|V_i - V_{rat}| \quad (5)$$

where $\overline{X}$ denotes the state vector. $R_i$, $P_i$ and $Q_i$ are the resistance, real power, and reactive power of branch i, respectively. $Nl$ is the total number of branches . $V_i$ and $V_{rat}$ are the real and rated voltage on bus i. $\lambda_1$ and $\lambda_2$ represent weighting factors. $\lambda_1 + \lambda_2 = 1$.

Owing to the DFIG operational requirements, the minimization of the objective function is subjected to the following constraints:

1) Distribution power flow equations:

$$P_i + P_{WFi} = P_{Di} + V_i \sum_{j=1}^{Nb} V_j (G_{ij} \cos\delta_{ij} + B_{ij} \sin\theta_{ij}) \quad (6)$$

$$Q_i + Q_{WFi} = Q_{Di} + V_i \sum_{j=1}^{Nb} V_j (G_{ij} \sin\delta_{ij} - B_{ij} \cos\theta_{ij}) \quad (7)$$

where $P_i$ and $Q_i$ are the substation injected active and reactive power at the ith bus. $P_{WFi}$ and $Q_{WFi}$ are the wind farm injected active and reactive power at the ith bus. $P_{Di}$ and $Q_{Di}$ are the active and reactive load power at the ith bus. $V_i$ and $V_j$ are the amplitude of voltage at the ith and jth bus, respectively. $G_{ij}$ and $B_{ij}$ are the conductance and the susceptance between the ith and jth nodes. $\delta_{ij}$ and $\theta_{ij}$ are the phase angle difference between the ith and jth nodes.

2) DFIG active capacity limits:

$$P_{gi.\min} \le P_{gi} \le P_{gi,\max} \quad (8)$$

where $P_{gi}$ , $P_{gi,\min}$ and $P_{gi,\max}$ are scheduled, minimum and maximum active power output of each i DFIG, respectively.

3) DFIG reactive capacity limits:

$$Q_{gi} \le \left| \sqrt{(3\frac{X_M}{X_S} U_S I_R)^2 - (P_{gi})^2} \right| - 3\frac{U_S{}^2}{X_S} \quad (9)$$

$$-Q_{gi} \le \left| \sqrt{(3\frac{X_M}{X_S} U_S I_R)^2 - (P_{gi})^2} \right| + 3\frac{U_S{}^2}{X_S}$$

where $Q_{gi}$ is reactive power output of each i DFIG wind turbine.

4) Node voltage magnitude limits:

$$V_{\min} \le V_i \le V_{\max} \quad (10)$$

where $V_i$ is the voltage magnitude of node i, $V_{\min}$ and $V_{\max}$ are low and upper bound of nodal voltage, respectively.

5) Distribution line limits:

$$\left| P_{ij}^{line} \right| < P_{ij,\max}^{line} \quad (11)$$

where $\left| P_{ij}^{line} \right|$ and $P_{ij,\max}^{line}$ are absolute power flowing over distribution lines and maximum transmission power between nodes i and j, respectively.

6) Radial structure of the network.

# 4 Particle swarm optimization

## 4.1 The standard PSO

The PSO is a population-based optimization method first proposed by Kennedy and Eberhart[16]. The PSO algorithm is initialized with the population of individuals being randomly placed in the search space and search for an optimal solution by updating individual generations. At each iteration, the velocity and the position of each particle are updated according to its previous best position (Pbesti) and the best position found by informants (Gbest). Each particle's velocity and position are adjusted by the following formula:

$$v_i^k(t) = \omega \cdot v_i^k(t) + c_1 \cdot r_1 (Pbest_i^k(t-1) - x_i^k(t-1)) + c_2 \cdot r_2 (Gbest^k(t-1) - x_i^k(t-1)) \quad (12)$$

$$x_i^k(t) = x_i^k(t) + v_i^k(t) \quad (13)$$

where $i$ is the number of the particle in the swarm, $k$ is the number of element in the particle $x_i(t)$, and $t$ is the iteration number. $v_i^k(t)$ and $x_i^k(t)$ are the velocity and the position of $k$th element of the $i$th particle at the $t$th iteration, respectively. $r_1$ and $r_2$ are the random numbers uniformly distributed between 0 and 1.The constants $c_1$ and $c_2$ are the weighting factors of the stochastic acceleration terms and $\omega$ is the positive inertia weight.

The suitable selection of inertia weight $\omega$ in (12) provides a balance between global and local explorations [17]. The inertia weight $\omega$ can be dynamically set with the following equation:

$$\omega^{(t+1)} = \omega^{\max} - \frac{\omega^{\max} - \omega^{\min}}{t_{\max}} \times t \quad (14)$$

In (14), $t_{\max}$ is the maximum number of iterations and $t$ is the current iteration number. $\omega$ often decreases linearly from about 0.9 to 0.4 during a run.

## 4.2 BPSO

The BPSO algorithm was introduced by Kennedy and Eberhart to allow the PSO algorithm to operate in binary problem spaces[18]. It uses the concept of velocity as a probability that a bit (position) takes on one or zero. In the BPSO, (12) for updating the velocity remains unchanged, but (13) for updating the position is re-defined by the rule

$$\begin{cases} x_i^k(t) = 1, & r < S(v_i^k(t-1)) \\ x_i^k(t) = 0, & r \ge S(v_i^k(t-1)) \end{cases} \quad (15)$$

where $S(v_i^k)$ is the sigmoid function for transforming the velocity to the probability as the following expression:

$$S(x) = \frac{1}{1+e^{-x}} \quad (16)$$

## 4.3 HPSOWM

The behavior of the PSO in the model presents some important aspects related with the velocity

update, if a particle's current position coincides with the global best position and if their previous velocities are very close to zero, then all the particles will stop moving, which may lead to a premature convergence of the algorithm known as stagnation. To avoid this problem, A new hybrid particle swarm optimization with wavelet mutation (HPSOWM) that incorporates a wavelet theory based mutation operation is proposed [19]. It applies the wavelet theory to enhance the PSO in exploring the solution space more effectively for a better solution.

The mutation operation is used to mutate the elements of particles. The proposed WM operation exhibits a fine-tuning ability. The details of the operation are as follows:

Every particle element of the swarm will have a chance to mutate that is governed by a probability of mutation $p_m \in [0\ 1]$, which is defined by the user. For each particle element, a random number between 0 and 1 will be generated such that if it is less than or equal to $p_m$, a mutation will take place on that element. For instance, if $x^k = [x_1^k, x_2^k \ldots x_i^k]$ is the selected kth particle, and the element of particle $x_i^k$ is randomly selected for the mutation the value of $x_i^k$ is inside the particle element's boundaries $[para_{\min}^i, para_{\max}^i]$, the resulting particle is given by $x^k = [x_1^k, x_2^k \ldots x_i^k]$ i.e.

$$\bar{x}_i^k(t) = \begin{cases} x_i^k(t) + \delta \times (para_{max}^k - x_i^k(t)) \ If \delta > 0 \\ x_i^k(t) + \delta \times (x_i^k(t) - para_{min}^k) \ If \delta \le 0 \end{cases} \quad (17)$$

where $i \in \{1, 2, \cdots, k\}$, k denotes the dimension of the particle, and $\delta$ is the mother wavelet.

There are many kinds of wavelets which can be used as a mother wavelet, such as the Harr wavelet, Meyer wavelet, Coiflet wavelet, Daubechies wavelet, Morlet wavelet and so on. These wavelets have different specificities. In this paper, the Morlet wavelet is chosen as the mother wavelet because the selected wavelet function offers the best performance. Its mathematical form is shown as follow:

$$\delta = = \frac{1}{\sqrt{a}} e^{-(\frac{\varphi}{a})^2/2} \cos(\omega_0(\frac{\varphi}{a})) \quad (18)$$

where $\omega_0$ is the central frequency of wavelet.

## 5 Joint optimization algorithm

In the proposed joint optimization algorithm, there are continuous and discrete control variables: the wind farm reactive power output $Q_{WF}$ and the status of switches $S_w$ .HPSOWM is utilized to optimize wind farm reactive power output, and BPSO is developed to find the optimal network structure for each particle updating instance at each iteration of wind farm reactive power output optimization algorithm.

The procedure of the joint optimization algorithm is given in Fig.5.

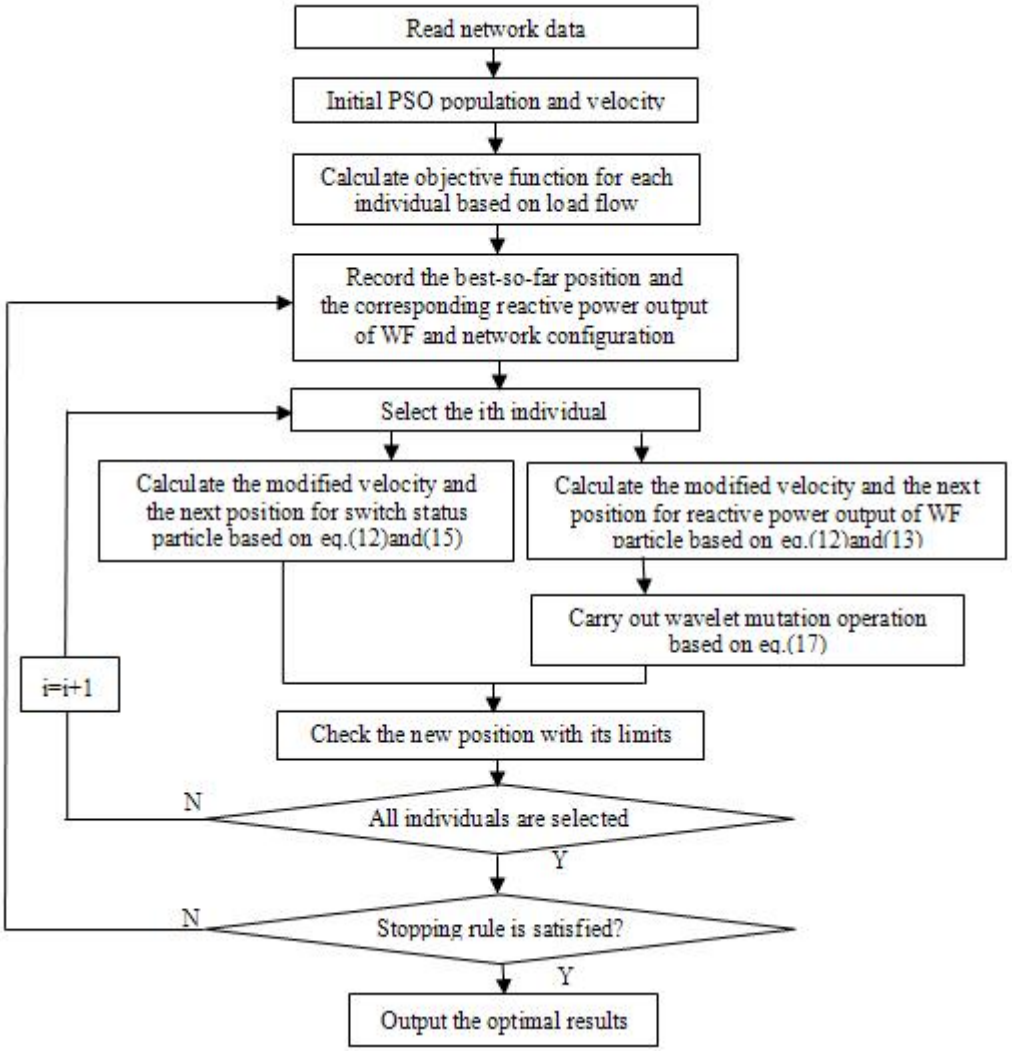


Fig.5. Flowchart of the proposed joint optimization algorithm

### 5.1 HPSOWM–based wind farm reactive power optimization

In this paper, the optimal reactive power output of wind farm is determined by having the reactive power output of wind farm as the control variable to be optimized in the HPSOWM optimization algorithm described in section 4.3.

In situations where the wind speed at each DFIG wind turbine is specified and the loads at buses are known, the active power generated by DFIG wind turbine can be calculated by means of the power curve. The total active power output of the wind farm is obtained by equation (3).Considering the DFIG capability limits, the maximum of the reactive power that each DFIG can generate or absorb is obtained. The total maximum reactive power output of the wind farm is obtained by equation (4). The steps followed for the implementation of the algorithm are described a follows:

Step 1. Using reactive power output of the wind farm as the control variable, generate an initial population randomly within the control variable bounds.

Step 2. Calculate objective function for each individual by using the result of distribution load flow.

Step 3. Perform mutation as described in Sections 4.3 to create new particle.

Step 4.Store the best individual of the current generation.

Step 5. Repeat step 2 to 4 till the termination criteria is met.

## 6 Simulation results

In this paper, the three feeder distribution system given in Ref.[20] is used to verify the validity and performance of the proposed joint optimization algorithm(see Fig.6). Test system has 13 sectionalizing branches and 3 tie branches, S15,S21,S26 are three tie switches. It is assumed that every branch has a sectionalizing switch and every tie switches are open in normal condition. The total power load is 28.7MW and 17.3MVAR. A small wind farm comprising 10 DFIG wind turbines of 660kW, with a power installed of 6.6MW is connected at node 12 through a rated 23/0.69 kV transformer. The performance parameters and the electric parameters of the studied 660kW DFIG wind turbine are given in Table 1 and Table 2[11].

### 6.1. Available active and reactive power in wind farm

Fig. 7 shows the wind speeds on the wind turbines considered in the simulation. In situations where the wind speed at each DFIG is specified, the real power output of DFIG can be calculated by means of the power curve.

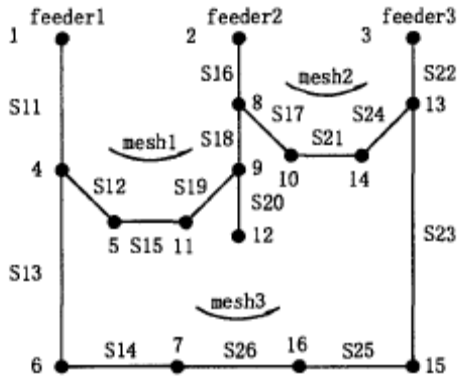


Fig.6. Three feeder distribution system

Table 1 DFIG Performance parameters

| PARAMETER | VALUE |
|---|---|
| Cut-in wind speed | 4 (m/s) |
| Cut-out wind speed | 25 (m/s) |
| Rated wind speed | 12.5 (m/s) |
| Rated voltage | 0.69 (kV) |

Table 2 DFIG electric parameters

| PARAMETER | VALUE |
|---|---|
| Rs, stator resistance per phase | 0.0067Ω |
| Xsl, stator leakage reactance per phase | 0.0300Ω |
| n, general turns ratio | 0.3806 |
| Xm, mutual reactance | 2.3161Ω |
| Rr, rotor resistance per phase | 0.0399Ω |
| Xsl, rotor leakage reactance per phase | 0.3490Ω |

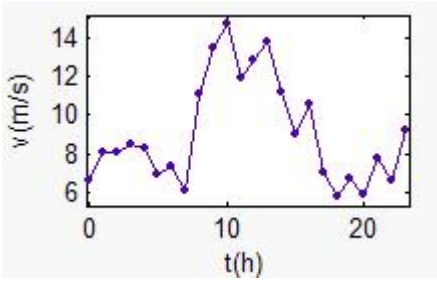


Fig.7. Curve of wind speed

It's assumed that the wind speed at each DFIG is the same, then the available power output of DFIG can be obtained(shown in Fig.8).

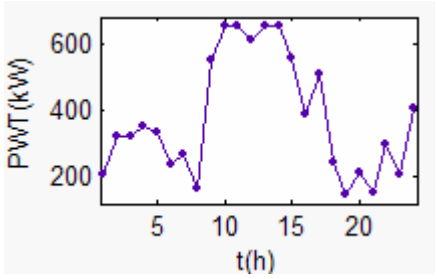


Fig.8.Active power of DFIG wind turbine

Considering the DFIG capability limits curve described in Fig.4, the maximum limit of available reactive power for each generated active power of DFIG wind turbine is obtained (shown in Fig.9).

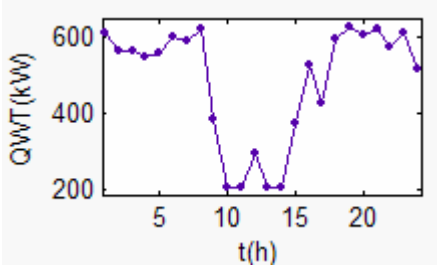


Fig.9. Maximum reactive power of DFIG wind turbine

available in wind farm. Generally, all of the

available active power in wind farm is fed into the distribution network.

From Fig.10, it can be observed that wind farm made up DFIG wind turbine can generate high quantities of reactive power when the available active power is far from its maximum. For example, in the period 1, wind speed is 5.8m/s, the active power wind farm generated is 1.4036MW, and the maximum reactive power wind farm can generate is 6.2619MVAR, which is much higher than others. But the maximum reactive power wind farm can generate become very low when the available active power is near its maximum. For example, in the period 6, wind speed is 14m/s, the active power wind farm generated is rated power 6.6MW, and the maximum reactive power DFIG can generate reduce to 2.0775MVAR.

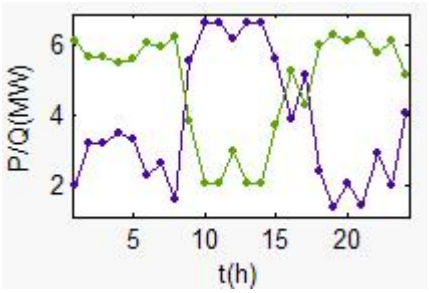


Fig.10. Active and reactive power available in wind farm

## 6.2 Joint optimization

For the proposed joint optimization algorithm, the number of particles is 20 and the given maximum iteration number of the algorithm is 100. The values of the parameters required for the implementation of the joint algorithm are c1 = c2 = 2.The upper and lower bounds of mutation probability are 0.001 and 0.3, respectively. The Morlet wavelet is chosen as the mutation wavelet parameter, which exhibits a fine-tuning ability.

Choosing period 3 as the example, in this period, the wind speed is 8.1m/s, the total active power wind farm generated is 3.1835MW, and the maximum available reactive power in wind farm is 5.658MVAR. To demonstrate the performance of the proposed joint optimization algorithm, the following five cases are studied. The optimization results of these five cases are given in Table 3.

Case 1) only perform network reconfiguration, power factor of the DFIG is 0.98.

Case 2) only perform wind farm reactive power optimization.

Case 3) perform network reconfiguration first, and then optimize wind farm reactive power.

Case 4) perform wind farm reactive power optimization first, and then carry out network reconfiguration.

Case 5) perform the proposed joint optimization algorithm.

As shown in Tab.3, the proposed joint optimization algorithm gets the lowest objective function value after optimization. Compared with original system, real power losses are reduced about 7%, from 0.345to 0.322MW. The optimization results of Cases 3 and 4 are better than that of Cases 1 and 2. It demonstrates that the joint of wind farm reactive power control and network reconfiguration can do a better job than only using wind farm reactive power control or network reconfiguration alone. The optimization result of Case 5 is better than that of Cases 3 and 4. It means that there is a mutual coupling relationship between wind farm reactive power control and network reconfiguration in the combined optimization. Choosing six available active and reactive power data from Fig.9, according to joint optimization algorithm proposed in this paper, the results of joint optimization is shown in Table 4.

To demonstrate the performance of the proposed joint optimization algorithm, the optimization results compared with the original system, which power factor of wind farm keep constant 0.98 (shown in Table 5).

Fig. 11 shows the power loss of the distribution system before and after optimization. In Fig. 11, the black bars represent the power loss after optimization, and the grey bars represent the power loss before optimization.

Fig.12 shows the minimum nodal voltage of the distribution system before and after optimization,

the line marked with circle represents the minimum nodal voltage after joint optimization, and the line marked with triangle represent the minimum nodal voltage before optimization.

From Figs. 11 and 12, we can find out that the proposed joint optimization algorithm can effectively reduce power loss and improve nodal voltage profile.

Table 3 Optimization results of different cases

| Case | PGWF(MW) | QGWF(MVAR) | Tie switch set | Objective function value | Loss(MW) | Mini.Nodal voltage(p.u.） |
|---|---|---|---|---|---|---|
| original system | 3.18 | 0.646 | 15, 21, 26 | 0.1896 | 0.345 | 0.978 |
| 1 | 3.18 | 0.646 | 17, 19, 26 | 0.1710 | 0.316 | 0.982 |
| 2 | 3.18 | 3.52 | 15, 21, 26 | 0.1711 | 0.364 | 0.985 |
| 3 | 3.18 | 2.33 | 17, 19, 26 | 0.1575 | 0.322 | 0.988 |
| 4 | 3.18 | 3.52 | 17, 19, 26 | 0.1617 | 0.336 | 0.985 |
| 5 | 3.18 | 2.07 | 17, 19, 26 | 0.1562 | 0.314 | 0.988 |

Table 4 Results of joint optimization of wind farm

| Case | PGWF(MW) | QGWF(MVAR) | Tie switch set | Objective function value | Loss(MW) | Mini.Nodal voltage(p.u.) |
|---|---|---|---|---|---|---|
| 1 | 1.40 | 3.97 | 17, 19, 26 | 0.1862 | 0.418 | 0.985 |
| 2 | 2.02 | 3.33 | 17, 19, 26 | 0.1754 | 0.380 | 0.985 |
| 3 | 3.18 | 2.07 | 17, 19, 26 | 0.1562 | 0.314 | 0.988 |
| 4 | 4.04 | 1.54 | 17, 19, 26 | 0.1471 | 0.288 | 0.985 |
| 5 | 6.13 | 0.81 | 17, 19, 26 | 0.1306 | 0.232 | 0.985 |
| 6 | 6.60 | 0.75 | 17, 19, 26 | 0.1280 | 0.224 | 0.985 |

Table 5 Original system

| Period | PGWF(MW) | QGWF(MVAR) | Tie switch set | Objective function value | Loss(MW) | Mini.Nodal voltage(p.u.) |
|---|---|---|---|---|---|---|
| 1 | 1.40 | 0.28 | 15, 21, 26 | 0.2356 | 0.431 | 0.973 |
| 2 | 2.02 | 0.41 | 15, 21, 26 | 0.2178 | 0.399 | 0.975 |
| 3 | 3.18 | 0.65 | 15, 21, 26 | 0.1896 | 0.345 | 0.978 |
| 4 | 4.04 | 0.82 | 15, 21, 26 | 0.1706 | 0.311 | 0.981 |
| 5 | 6.13 | 1.24 | 15, 21, 26 | 0.1349 | 0.247 | 0.985 |
| 6 | 6.60 | 1.34 | 15, 21, 26 | 0.1317 | 0.236 | 0.986 |

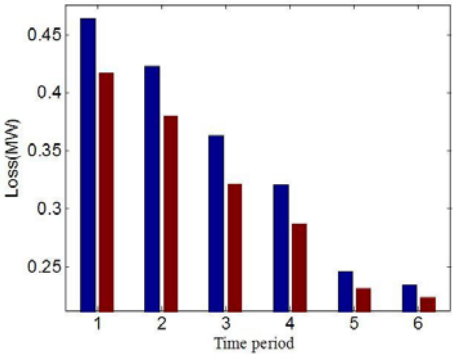


Fig.11. Power loss of the distribution system

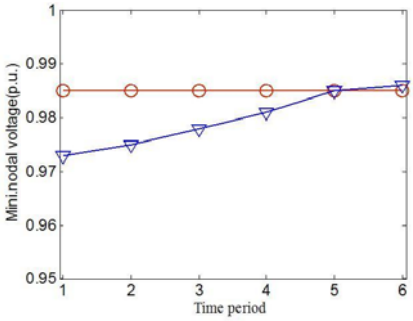


Fig.12. Minimum nodal voltage of the distribution system

## 7. Conclusions

In this paper, a joint optimization algorithm of combining reactive power control of wind farm and network reconfiguration is proposed. In the proposed joint optimization algorithm, reactive power output of wind farm and status of switches are utilized as the control variable for losses minimization and voltage profile improvement. The optimal reactive power output of wind farm and the optimal network structure are efficiently obtained by taken in account DFIG reactive capability limits in the simulation. From the results obtained in the simulations, it can be concluded that wind farm made up of DFIG can constitute an important continuous reactive power source to support system voltage control. The simulation results also shown that the jointly optimization get better solution results than using the reactive power control optimization algorithm or the network reconfiguration algorithm alone.

*References:*

[1] J.M. Rodriguez, J.L. Fernandez, D. Beato, et, al., Incidence on Power System Dynamics of High Penetration of Fixed Speed and Doubly Fed Wind Energy Systems: Study of the Spanish Case, IEEE Transactions on Power Systems,Vol.17, No.4, 2002, pp.1089-1095.

[2] M. Korpaas, A.T. Holen, R. Hildrum, Operation and Sizing of Energy Storage for Wind Power Plants in a Market System, International Journal of Electrical Power & Energy Systems, Vol.25, No.8, 2003, pp.599-606.

[3] H. Lund, Large-scale Integration of Wind Power into Different Energy Systems, Energy,Vol.30, No.13, 2005, pp.2402-2412.

[4] H. Lund, E. Münster, Modelling of Energy Systems with a High Percentage of CHP and Wind Power , Renewable Energy, Vol. 28,No. 14, 2003, pp.2179-2193.

[5] A.Tapia, G. Tapia, J. X. Ostolaza, J.R. Saenz, R. Criado, J. L. Berasategui, Reactive Power Control of a Wind Farm made up with Doubly Fed Induction Generators (I), IEEE Porto Power Tech Conference, Porto, Portugal, September 2001.

[6] D. Santos-Martin, S. Arnaltes, J.L.R. Amenedo, Reactive Power Capability of Doubly Fed Asynchronous Generators, Electric Power

Systems Research, Vol.78, No.11, 2008, pp.1837–1840.

[7] D. J. Atkinson, R. A. Lakin, and R. Jones, A Vector-Controlled Doubly-Fed Induction Generator for a Variable-speed Wind Turbine Application, Transactions of the Institute of Measurement & Control, Vol.19, No.1, 1997, pp.2–12.

[8] R. S. Peña, J. C. Clare, and G. M. Asher, Vector Control of a Variable Speed Doubly-fed Induction Machine for Wind Generation Systems, EPE Journal,Vol.6, No.3, 1996, pp.60–67.

[9] G. Tapia, A. Tapia, J.X. Ostolaza, Two Alternative Modeling Approaches for the Evaluation of Wind farm Active and Reactive Power Performances, IEEE Transactions on Energy Conversion, Vol.21, NO. 4, 2006, pp.909-920.

[10] R.G. de Almeida, E.D. Castronuovo, J.A.P. Lopes, Optimum Generation Control in Wind farms When Carrying Out System Operator Requests, IEEE Transactions on Power Systems PWRS, Vol. 21, No. 2, 2006, pp.718-726.

[11] A.Tapia , G. Tapia, J.X. Ostolaza, Reactive Power Control of Wind Farms for Voltage Control Applications, Renewable Energy, Vol.29, No.3, 2004, pp.377–392.

[12] D. Santos-Martin, S. Arnaltes, J.L.R. Amenedo, Reactive power capability of doubly fed asynchronous generators, Electric Power Systems Research, Vol.78, No.11, 2008, pp.1837–1840.

[13] C.F. Moyano, J.A.P. Lopes, An Optimization Approach for Wind Turbine Commitment and Dispatch in a Wind Park, Electric Power Systems Research,Vol.79,No.1,2009,pp.71–79.

[14] D. Zhang, Z.C. Fu, and L.C. Zhang, Joint Optimization for Power Loss Reduction in Distribution Systems, IEEE Transactions on Power Systems ,Vol.23, No. 1, 2009, pp.161-169.

[15] L.M. Fernández, C.A. García, J.R. Saenz, F. Jurado, Aggregated Dynamic Model for Wind Farms with Doubly Fed Induction Generator Wind Turbines, Renewable Energy, Vol.33, No.1,2008, pp.129-140.

[16] J. Kennedy, R. Eberhart, Particle Swarm Optimization, IEEE International Conference on Neural Networks, Perth ,Australia, Nov/Dec 1995, pp.1942-1948.

[17] Y. Shi, R. Eberhart, A Modified Particle Swarm Optimizer, Proceeding of the IEEE World Congress on Computational Intelligence, Anchorage, AK, USA, May 1998, pp. 69–73.

[18] J. Kennedy,R. Eberhart, A Discrete Binary Version of The Particle Swarm Algorithm, Proceeding of the IEEE World Congress on Computational Cybernetics and Simulation , Piscataway, NJ,1997 pp.4104–4108.

[19] S.H. Ling, H.H.C. Iu, K.Y. Chan, et, al. Hybrid Particle Swarm Optimization with Wavelet Mutation and Its Industrial Applications. IEEE Transactions on Systems, Man and Cybernetics, Vol.38, No. 3, 2008, pp.743–764.

[20] S. Civanlar, J. J. Grainger, H. Yin, et,a1., Distribution Feeder Reconfiguration for Loss Reduction,IEEE Trans Delivery,Vol.3, No.7, 2008, pp.1217-1223.